catalysts

MDPI

Article

Effect of Acid Properties of Fluorinated Beta and ZSM-5 Zeolites Used as Supports of Ni Catalysts for the Catalytic Hydrodeoxygenation of Guaiacol

Gabriela Quintero-Arroyo [1,2], Angie C. Rueda [1], Judith Granados-Reyes [1], Jayson Fals [2] and Yolanda Cesteros [1,*]

[1] Departament de Química Física i Inorgànica, Universitat Rovira i Virgili, 43007 Tarragona, Spain; gabriela.quintero@estudiants.urv.cat or gquinteroa@mail.uniatlantico.edu.co (G.Q.-A.); angiecarolyne.rueda@urv.cat (A.C.R.); judithcecilia.granados@urv.cat (J.G.-R.)

[2] Grupo de investigación en Oxi/Hidrotratamiento Catalítico y Nuevos Materiales, Programa de Química-Ciencias Básicas, Universidad del Atlántico, Barranquilla 080003, Colombia; jaysonfals@mail.uniatlantico.edu.co

* Correspondence: yolanda.cesteros@urv.cat; Tel.: +34-977559571

Abstract: Commercial NH_4-Beta and Na-ZSM-5 zeolites were fluorinated with different amounts of NH_4F and using different procedures (room temperature, conventional refluxing, microwave refluxing). Samples were characterized by XRD, N_2 physisorption, FTIR, ^{1}H NMR, SEM-EDS, and TGA of adsorbed cyclohexylamine. An increase in the concentration of NH_4F led to fluorinated zeolites with higher surface areas and slightly lower amounts of Brønsted acid sites due to some dealumination. Fluorination by conventional or microwave refluxing at shorter times did not dealuminate ZSM-5, resulting in the formation of higher particle sizes. Ni/fluorinated beta catalysts were more active than Ni/fluorinated ZSM-5 catalysts for the hydrodeoxygenation of guaiacol at 180 °C and 15 bar of H_2 for 1 h due to their higher amount of acid sites. The appropriate proportion of metallic and Brønsted acid centers allowed for the selective obtention of cyclohexane (58%) for the Ni supported on beta fluorinated with NH_4F 0.1 M catalyst. The combination of this fluorinated beta to a Ni/ordered mesoporous carbon catalyst significantly boosted its selectivity to cyclohexane from 0 to 65%. Fluorinated ZSM-5 samples, although having stronger Brønsted acid sites, as observed by ^{1}H NMR, they had lower amounts, leading to higher selectivity to cyclohexanol when used as catalytic supports.

Keywords: zeolites; Ni catalysts; fluorination; microwaves; guaiacol hydrodeoxygenation; cyclohexane

Citation: Quintero-Arroyo, G.; Rueda, A.C.; Granados-Reyes, J.; Fals, J.; Cesteros, Y. Effect of Acid Properties of Fluorinated Beta and ZSM-5 Zeolites Used as Supports of Ni Catalysts for the Catalytic Hydrodeoxygenation of Guaiacol. *Catalysts* **2024**, *14*, 586. https://doi.org/10.3390/catal14090586

Academic Editors: Diego Luna, Sergio Carrasco and Rebeca Martínez-Haya

Received: 31 July 2024
Revised: 25 August 2024
Accepted: 26 August 2024
Published: 2 September 2024

1. Introduction

The demographic and economic growth in recent decades has created a greater demand for energy, both in productive activities and among the general population seeking increased comfort. This reality is compounded by the high consumption of fossil resources, which causes significant environmental impact. This challenge motivates us to optimize production technologies for biofuels and high-value chemicals using renewable sources like biomass, offering a more sustainable and environmentally friendly alternative [1–3]. Lignocellulosic biomass is one of the most abundant and sustainable sources to produce biofuels. This biomass, which is mainly composed of cellulose, hemicellulose, and lignin, can be converted into liquid fuels through various fractionation and refining processes. Its abundance and ability to be transformed into high-value products position it as a promising alternative to fossil fuels, contributing significantly to the reduction in greenhouse gas emissions and the mitigation of climate change. Furthermore, the use of lignocellulosic biomass can boost the development of rural economies and create new opportunities in the agricultural and forestry sectors [4,5].

To produce sustainable liquid fuels from biomass, it is essential to transform these oxygen-rich compounds into hydrocarbons. The aromatic units present in lignin can be thermally and catalytically decomposed into various compounds of interest, including guaiacol, which is characterized by its high oxygen content, high viscosity, instability, and tendency to polymerization. The conversion of lignin model compounds such as anisole, catechol, and guaiacol through cracking or hydrodeoxygenation (HDO) reactions represents a promising route to exploit lignin in the production of biofuels and other valuable products [6–8].

The catalysts used in HDO reactions are mainly composed of two functional parts: a redox (metal) component and acidic sites. The redox component, usually noble metals such as Ru, Re, and Pd, and other transition metals such as Ni, plays an important role in facilitating hydrogen transfer reactions necessary to remove oxygen in organic compounds. The acidic sites, in contrast, are responsible for the activation and cleavage of chemical bonds within oxygen-containing molecules. This synergistic combination of redox and acidic functions allows efficient conversion of oxygen-rich lignocellulosic compounds into stable hydrocarbons [9].

Different metals supported on oxides or zeolites have been used for the hydrodeoxygenation of guaiacol, mostly at high temperatures (>200 °C) and H_2 pressures (40–50 bar). Hellinger et al. studied the use of Pt supported on metal oxides and zeolites for this reaction [10]. They found that the deoxygenation capacity of the catalysts improved when Pt particles were deposited on the acidic zeolites. Later, Wang et al. [11] confirmed the influence of the acid support structure on the dispersion and accessibility of active sites using Pd supported on micro and mesoporous H-ZSM-5 zeolites. Studies using zeolites as supports of Ni, a low-cost metal with high hydrogenation activity, have also been reported. Gutierrez et al. [12] obtained deoxygenated compounds, mainly cyclohexane (78%) at 95% conversion of guaiacol at 220 °C with 40 bar H_2 pressure using Ni_2P deposited on different ZSM-5 lamellar and pillared ZSM-5 zeolites. Li et al. also tested Ni metal supported on acid hierarchical ZSM-5 zeolites, obtaining a selectivity of 90% towards cyclohexane at 100% conversion of guaiacol at 240 °C with 40 bar H_2, concluding that once again, tunneling the acid and structural properties of the support could promote both deoxygenation and aromatic ring hydrogenation [13].

Several authors reported that the guaiacol HDO activity of supported metal catalysts can be improved by incorporating additional Brønsted acid sites, usually H-zeolites, through a synergetic effect between metallic and acid sites [14–17]. Wang et al. studied the hydrodeoxygenation of guaiacol to cyclohexane at lower temperatures (140 °C) over a Ni/SiO_2 catalyst combined with H-β zeolite [14], resulting in a 91.7% yield of cyclohexane. The acidity of the H-β zeolite had a significant impact on the selective obtention of cyclohexane. In a previous work, we obtained 78% of selectivity to cyclohexane when combining a Ni/ordered mesoporous carbon with a H-β zeolite at 180 °C, 30 bar of H_2 for 1 h [18]. The main reaction products obtained for the HDO of guaiacol at reaction temperatures below 200 °C and the type of reactions involved are indicated in Scheme 1.

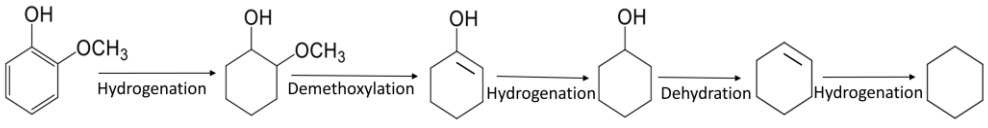

Scheme 1. Catalytic hydrodeoxygenation of guaiacol at low reaction temperatures.

Zeolites are widely used as catalyst supports due to their tunable acidity, porosity, and shape selectivity. One way to modify the acidity of the zeolites is their fluorination through the post-synthesis treatment with an aqueous solution of NH_4F and later calcination [19]. The incorporation of the fluorine in the zeolite framework can increase the Brønsted acidity of the resulting H^+ that are interacting with the framework [19].

This work aimed to study the effect of different fluorination techniques on the acidic properties of ZSM-5 and beta zeolites with the objective to use these fluorinated zeolites as catalytic supports of Ni catalysts or combined with a Ni/ordered mesoporous carbon for the hydrodeoxygenation of guaiacol under mild reaction conditions: 180 °C and 15 bar of H_2 for 1 h.

2. Results and Discussion

2.1. Characterization of the Catalytic Supports and the Catalysts

Table 1 shows the main characterization data of the fluorinated supports. Some slight dealumination was observed for the ZSM-5 samples fluorinated at room temperature with different NH_4F concentrations, 0.1 M (ZF), 0.2 M (ZF0.2), and 0.05 M (ZF0.05), for a long time (42 h) since they showed slightly higher Si/Al ratios and a shift to higher values of the IR bands assigned to symmetric and asymmetric stretching of the T-O bond (T = Si, Al) than their corresponding commercial one (Table 1). This trend was more marked for the sample fluorinated with the highest concentration of NH_4F (ZF0.2). The fact that the Si-O bond is shorter than the Al-O bond, and Al has lower electronegativity than Si, explains the increase in the strength of the T-O bond (T = Si, Al) under dealumination conditions [20,21]. However, for the ZSM-5 samples fluorinated at 40 °C for 4 h by conventional refluxing (ZFR) or by microwave refluxing (ZFMwR), dealumination practically did not occur, as concluded from the XRF and IR results obtained for these samples (Table 1). This can be explained by the shorter fluorination time used.

Table 1. Characterization of the fluorinated zeolites.

Samples	Si/Al (XRF)	IR Bands (cm^{-1}) [a]		Langmuir Surface Area (m^2/g) [b]	Acidity (mmol H^+/g) [c]
		υ_1	υ_2		
Z	20.0	1058	795	505	0.25
ZF	20.5	1061	795	549	0.37
ZF0.2	21.6	1071	795	558	0.33
ZF0.05	20.3	1060	795	516	0.27
ZFR	20.1	1059	798	457	0.39
ZFMwR	20.1	1053	797	454	0.45
B	12.5	1047	792	630	0.30
BF	14.6	1064	795	731	0.51
BF0.2	15.2	1066	797	767	0.29
BF0.05	13.8	1050	793	724	0.48
HB	13.2	1054	795	636	0.60
HBF	14.1	1065	798	702	0.58

[a] Frequencies of the main asymmetric stretch (υ_1) and the main symmetric stretch (υ_2) due to the T-O bond (T = Si, Al); [b] from nitrogen physisorption results; [c] determined by TGA of desorbed cyclohexylamine.

On the other hand, fluorinated beta samples showed higher partial dealumination since all of them had higher Si/Al ratios, confirmed by the shift to higher values of the IR bands (Table 1). Again, higher concentrations of NH_4F led to higher dealumination. The differences observed between these zeolites can be related to the flexibility of each zeolite framework and the accessibility of the aluminium atoms, depending on the pores' arrangement and sizes. Thus, beta zeolites have a three-dimensional 12-ring pore system (straight channels of diameter 6.6 × 6.7 Å and sinusoidal channels of diameter 5.6 × 5.6 Å), whereas ZSM-5 zeolites have a three-dimensional 10-ring pore system with channels of diameter 5.1 × 5.5 Å. These results agree with those that previously reported the lower dealumination of the ZSM-5 zeolites when compared with beta zeolites [21].

Zeolite modification by fluorination with NH_4F practically did not affect the zeolite structure (Figure 1); however, some decrease in crystallinity was observed for all samples, especially for beta samples (e.g., Figure 1), due to the characteristics of its structure, as commented above. Interestingly, the ZSM-5 sample fluorinated by microwaves (ZFMwR) displayed higher crystallinity than the sample fluorinated by conventional heating prepared

at the same conditions (ZFR) (Figure 1). This could be related to the effect of microwaves, which enhances the growth of crystals [22].

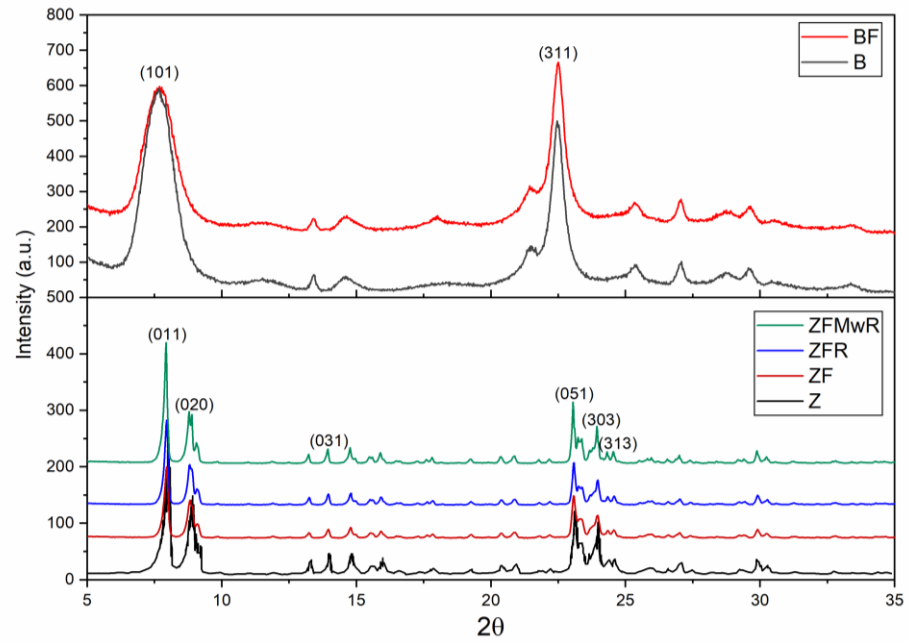

Figure 1. XRD of representative fluorinated ZSM-5 and beta samples.

Nitrogen adsorption-desorption isotherm shapes of the fluorinated samples were similar to those of their corresponding commercial ones (Figure 2), identified as type I corresponding to microporous materials, according to the Brunauer, Deming, Deming, and Teller classification [23], and characteristics of this type of zeolite.

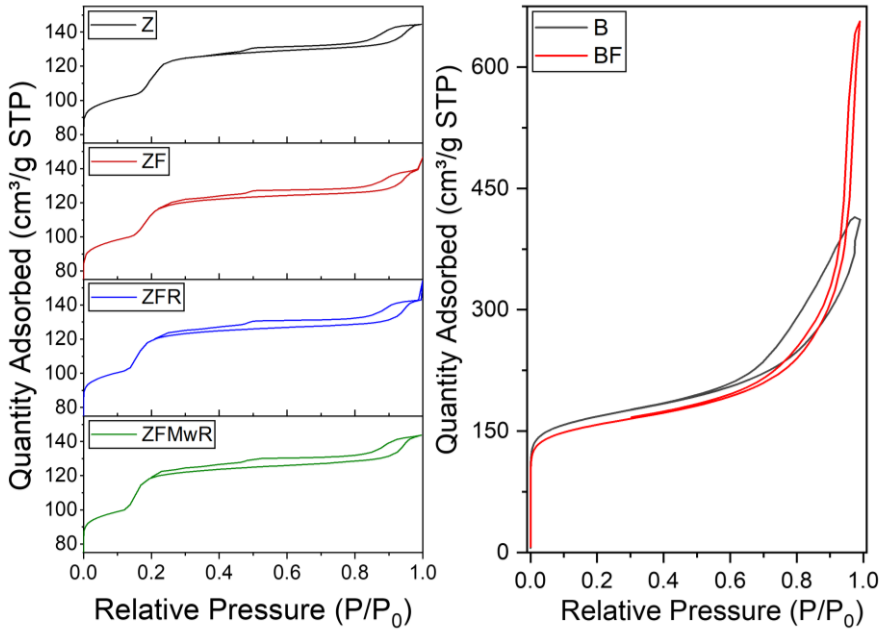

Figure 2. N_2 adsorption-desorption isotherms of representative fluorinated ZSM-5 and beta samples.

The two plateaus of the N_2 adsorption-desorption isotherms of ZSM-5 samples have been attributed to two different states of the adsorbed nitrogen, a liquid-like and a solid-like phase, respectively [24,25]; however, the explanation of close packing of the nitrogen molecules at the intersections of the channels has also been suggested [26].

The surface areas of the samples fluorinated at room temperature at longer times were slightly higher than those of the commercial ZSM-5 and Beta, respectively (Table 1). This can be due to some mesoporosity generated due to the slight dealumination suffered by these fluorinated samples (Table 1). However, for the samples fluorinated with temperature at shorter times (ZFR and ZFMwR) the surface areas decreased compared to the commercial one. This could be related to the variations of crystallinity observed for these samples, which practically did not show dealumination.

Scanning electron microscopy with energy dispersive X-ray spectroscopy (SEM-EDS) allowed us to confirm the presence of fluorine in the fluorinated samples (e.g., Figure 3 left).

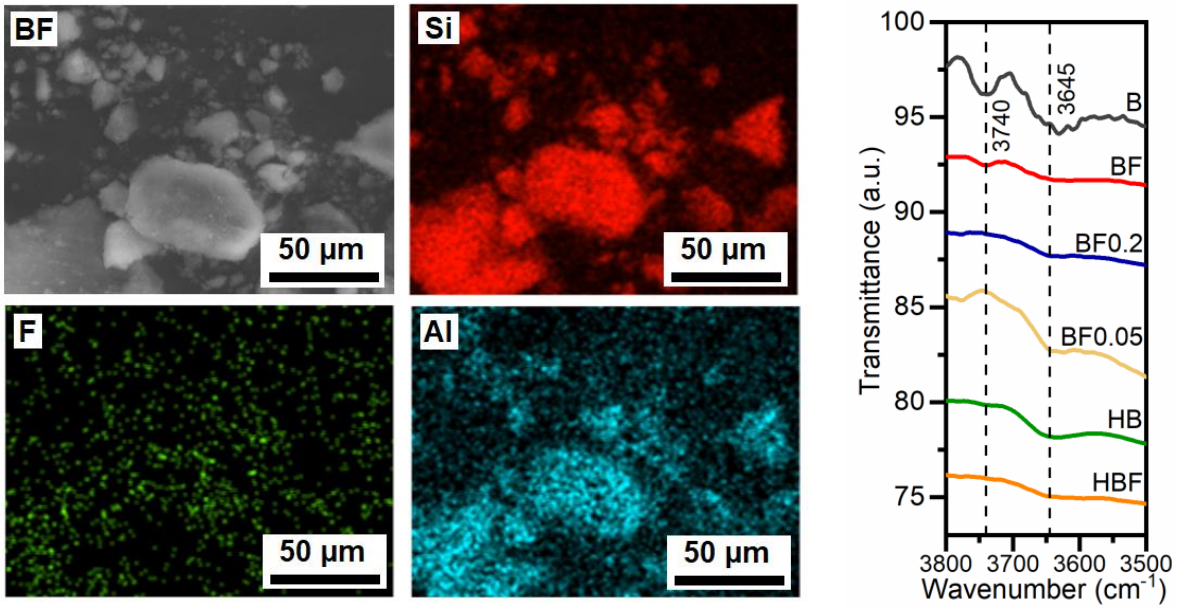

Figure 3. (**Left**) SEM-EDS of sample BF, and (**right**) infrared spectra of the fluorinated beta samples in the region 3800–3500 cm^{-1}.

The FTIR spectra in the region between 3800 and 3500 cm^{-1} was carefully analyzed for the fluorinated beta samples to observe possible variations due to the presence of the fluorine (Figure 3, right). Two peaks were observed at 3740 and 3645 cm^{-1} for the non-fluorinated sample (B). The first corresponds to SiOH terminal groups and the second corresponds to SiOHAl groups; however, the presence of silanol groups related to structural defects cannot be discarded [27–29]. After fluorination, the position of the band at 3645 cm^{-1} practically did not change, while the band at 3740 cm^{-1} shifted to 3785 cm^{-1} for several samples. This has been attributed to the presence of low acidity OH groups bonded to extra-latice aluminium. The IR profile for the samples HB and HBF were very similar. This means that although fluorine is present in the sample, it probably was not incorporated in the zeolitic structure.

The SEM technique was also used to monitor the effect of the different methodologies used for the fluorination of ZSM-5 with NH_4F 0.1 M on the morphologies and particle size distribution of the fluorinated samples (Figure 4). The use of temperature by refluxing during fluorination (ZFR and ZFMwR) resulted in the formation of higher particle sizes (7–12 µm), with more homogeneous distribution for the samples heated by conventional refluxing (ZFR), maintaining the geometry of the starting zeolite particles. However, the use of longer fluorination times at room temperature led to smaller particles (5–6 µm) with a loss in the definition of the geometrical aspect (Figure 4).

Table 1 depicts the amount of Brønsted acid sites determined for all samples by thermogravimetry of desorbed cyclohexylamine, while Figure 5 shows the ^1H NMR spectra for several representative ZSM-5 and beta samples.

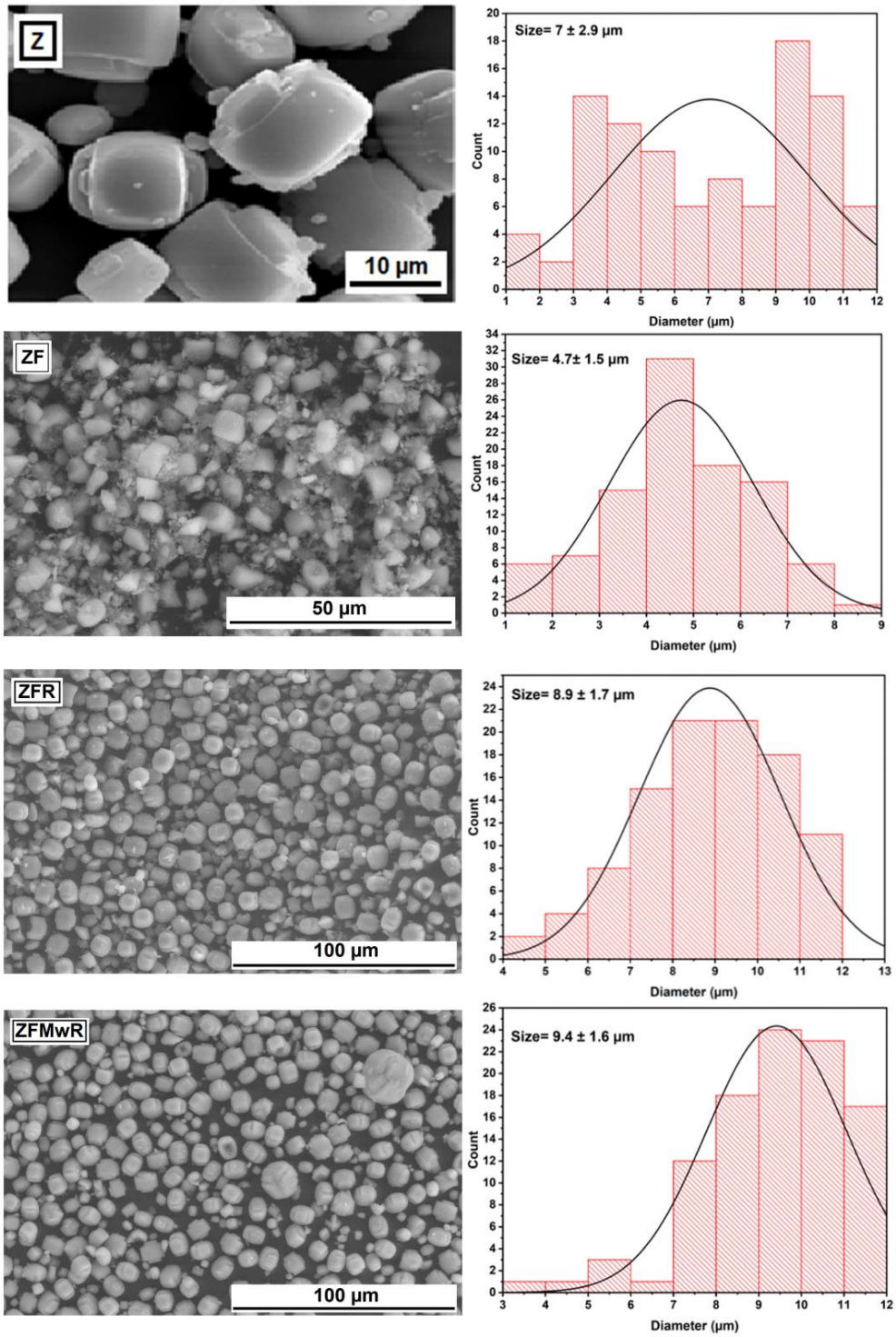

Figure 4. Scanning electron micrographs of several fluorinated ZSM-5 samples.

Practically all fluorinated zeolites showed higher amounts of Brønsted acid centers than their corresponding starting zeolites, as expected. In the case of commercial Na-ZSM-5, during fluorination with NH_4F in addition to the incorporation of fluorine, Na^+ cations were exchanged by NH_4^+, which after further calcination at 450 °C for 5 h, resulted in the formation of H^+, compensating for the negative charge of the zeolite framework. For NH_4-Beta, during the calcination step, carried out after fluorination, H^+ were formed. The small differences observed in the amount of Brønsted acid centers between fluorinated zeolites could be related to the slight partial dealumination observed for these samples,

since low amounts of Al in the zeolite structure involve less cations compensating for the negative framework charge and, therefore, lower amounts of H^+.

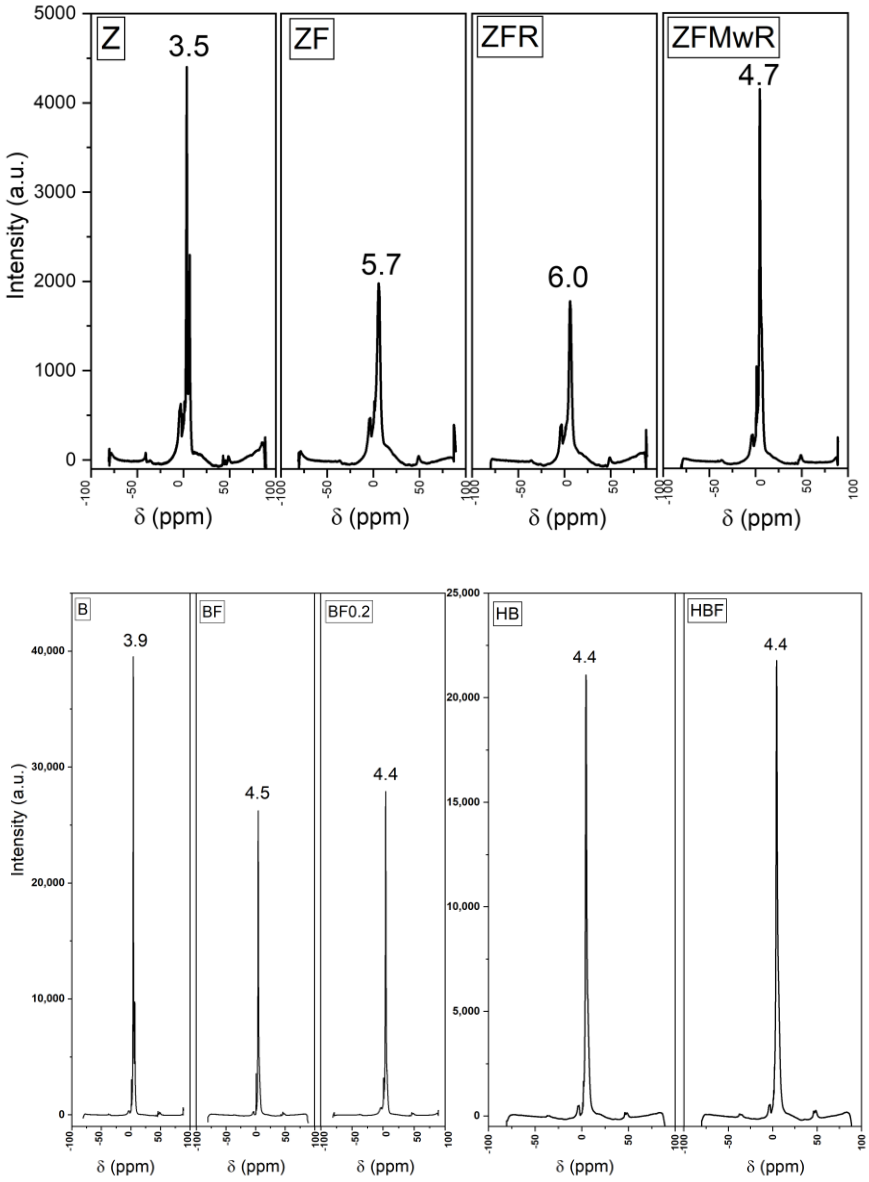

Figure 5. ^{1}H NMR of several fluorinated ZSM-5 and beta samples.

The ^{1}H NMR technique has been postulated as a useful technique to determine the presence of different kinds of hydroxyl groups in zeolites and, therefore, to evaluate their Brønsted acidity strength [30–32]. For commercial Na-ZSM-5 and NH_4-Beta zeolites, one ^{1}H NMR peak at 3.5 and 3.9 ppm, respectively, was observed (Figure 5). This peak can be associated to free Brønsted protons, as previously reported [32]. When ZSM-5 was fluorinated by treatment with NH_4F 0.1 M using different methodologies (samples ZF, ZFR, and ZFMwR) and later calcined, a clear shift of the peak to higher ppm values was observed in all cases (Figure 5). This peak should be attributed to the Brønsted protons formed during calcination, which are interacting with the zeolite framework. This means that fluorinated ZSM-5 samples had stronger Brønsted acid sites. This can only be explained by an inductive effect by F, confirming the introduction of fluorine atoms in the zeolite framework.

The different amount of acid sites observed for ZF, ZFR, and ZFMwR (Table 1) should be related to the protons formed during calcination; however, the presence of surface-

defective sites should not be discarded. An increase in the NH_4F concentration slightly decreased the number of Brønsted acid sites (Table 1), as expected, due to the slightly higher zeolite dealumination detected (Table 1).

On the other hand, for fluorinated beta samples, an increase in the concentration of NH_4F used during the treatment did not affect the strength of the protons, which had similar values (4.4–4.5 ppm) (Figure 5); however, the amount of acid centers decreased by increasing the NH_4F concentration used due to the higher dealumination (Table 1).

XRD patterns of Ni/fluorinated ZSM-5 catalysts showed the presence of a totally reduced crystalline Ni phase in addition to the peak characteristics of the zeolite (Figure 6). In contrast, unreduced crystalline NiO together with crystalline Ni and zeolite characteristic peaks were observed in the XRD patterns of the Ni/fluorinated beta catalysts (Figure 7). This should be related to a higher interaction of NiO with the beta support.

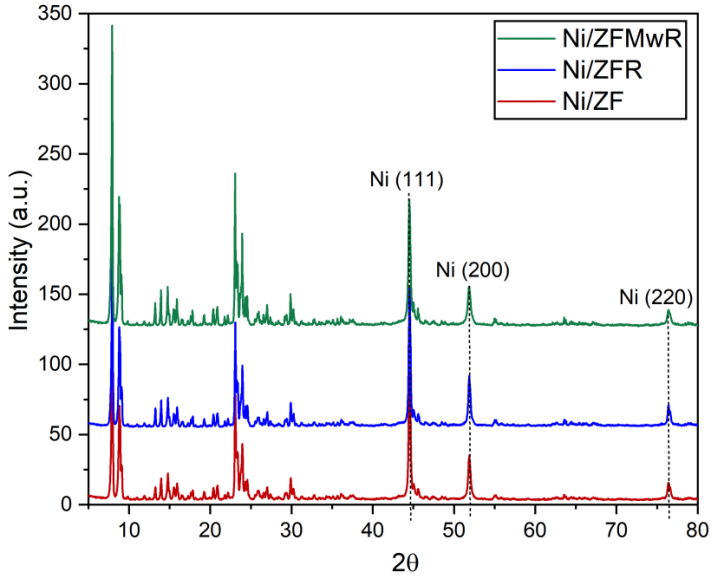

Figure 6. XRD patterns of several Ni/fluorinated ZSM-5 catalysts.

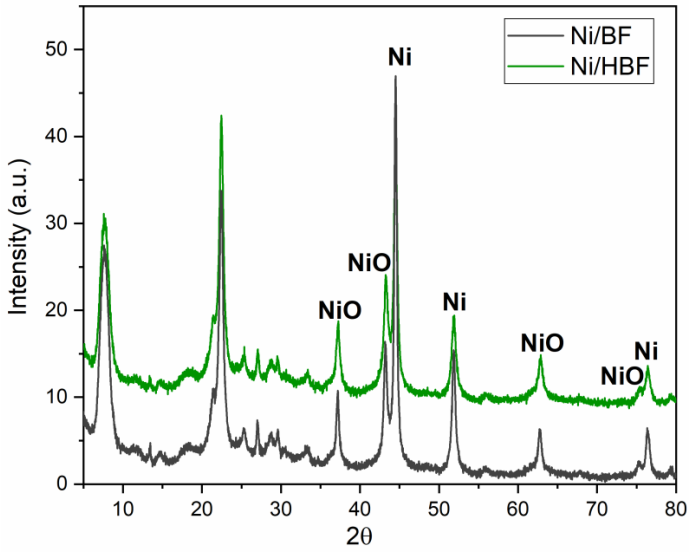

Figure 7. XRD patterns of several Ni/fluorinated beta catalysts.

2.2. Catalytic Activity

Figure 8 shows the catalytic activity of the Ni/fluorinated ZSM-5 for the hydrodeoxygenation of guaiacol at 180 °C, 15 bar of H_2 pressure for 1 h. All catalysts were active

for this reaction with low-moderate conversion values (22–48%). The main reaction product was methoxycyclohexanol (50–73%). These results indicate that these catalysts had a high hydrogenating ability since this reaction product was fully hydrogenated. However, demethoxylation and later dehydration was not totally achieved. This catalytic result agrees with the results obtained by other supported nickel catalysts for this reaction [33–35], especially at reaction temperatures below 200 °C [14,15,18]. Cyclohexane and cyclohexanol were obtained in low-moderate amounts, with a maximum of 18% of cyclohexane for the catalyst Ni/ZF and 25% of cyclohexanol for the catalyst Ni/ZFR. This could be explained by the higher amount and, especially, the higher strength of the Brønsted acid sites of these catalytic supports (Figure 5), which should favor demethoxylation and dehydration reactions.

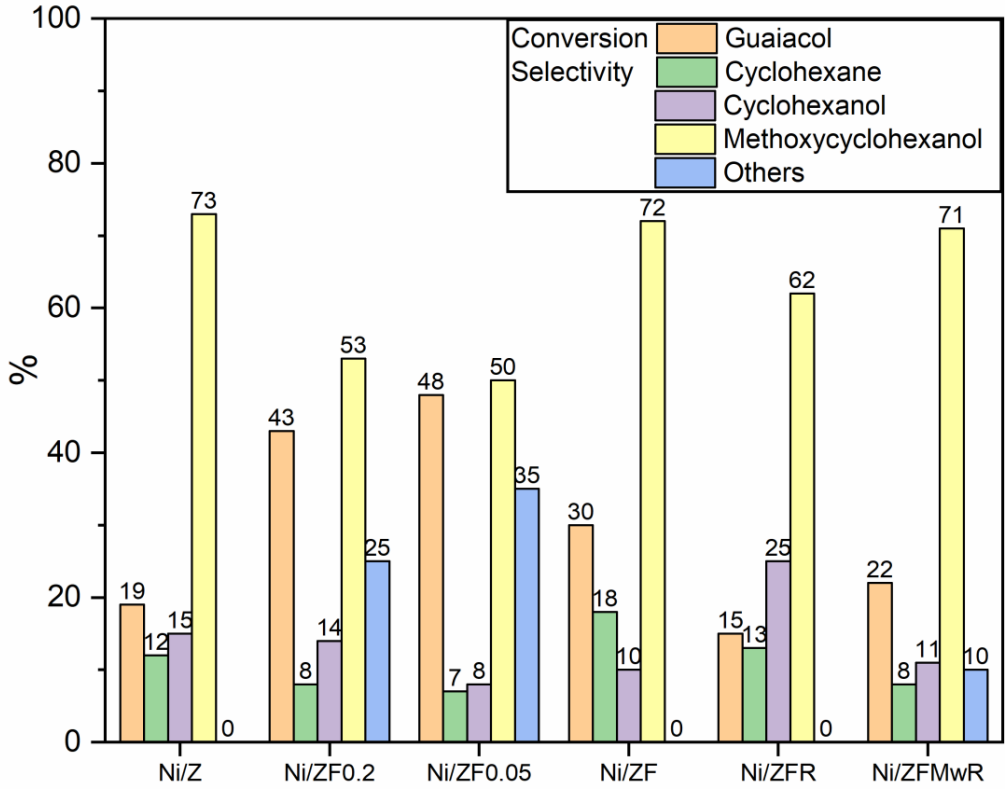

Figure 8. Catalytic activity of the Ni/fluorinated ZSM-5 catalysts. Reaction conditions: 200 mg of guaiacol; 100 mg of catalyst; H_2, 15 bar; reaction time, 1 h; reaction temperature, 180 °C; solvent, dodecane.

To increase the accessibility of the acid sites, and then, favor the demethoxylation and dehydration reactions for the formation of higher amounts of cyclohexane and cyclohexanol, two Ni/ZF catalysts were prepared with less Ni content (10 wt% and 20 wt%). However, by decreasing the Ni content, the selectivity to cyclohexane and cyclohexanol decreased (Figure 9), mainly at the expense of the formation of higher amounts of other products. For the most part, these other products were detected at lower reaction times in the chromatograph, so this means that an increase in the accessibility of the Brønsted acid sites favored other acid-catalyzed reactions, such as the formation of cracking products.

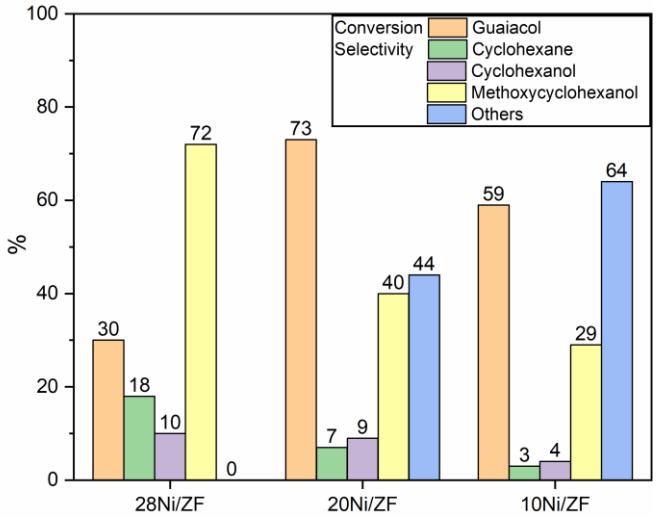

Figure 9. Catalytic activity of the Ni/ZF catalysts with different Ni contents. Reaction conditions: 200 mg of guaiacol; 100 mg of catalyst; H_2, 15 bar; reaction time, 1 h; reaction temperature, 180 °C; solvent, dodecane.

Figure 10 shows the catalytic activity results of the Ni/fluorinated beta for the hydrodeoxygenation of guaiacol at 180 °C, 15 bar of H_2 pressure for 1 h. These catalysts were more active than Ni/fluorinated ZSM-5 catalysts with conversion values between 78% and 100%. This can be explained by the higher amount of Brønsted acid sites of these catalysts (Table 1), together with the presence of additional acidity due to the unreduced NiO (Figure 7), which can also be responsible for the higher amounts of other products formed (Figure 10). Interestingly, the Ni/BF catalysts showed the appropriate proportion of metallic and Brønsted acid centers, which allowed the obtention of a high selectivity to cyclohexane (58%) for a 96% of conversion. This is the best catalytic result reported in the literature for a supported Ni catalyst at mild reaction conditions, since they usually yielded methoxycyclohexanol as the main product [14–18].

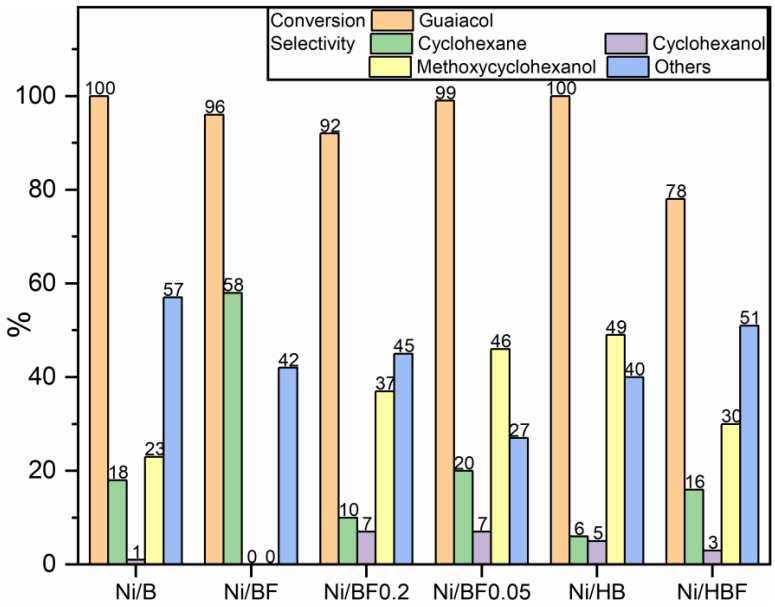

Figure 10. Catalytic activity of the Ni/fluorinated Beta catalysts. Reaction conditions: 200 mg of guaiacol; 100 mg of catalyst; H_2, 15 bar; reaction time, 1 h; reaction temperature, 180 °C; solvent, dodecane.

For this reason, there are several studies in which materials are combined with metal supported catalysts, giving additional Brønsted acid sites, usually H-zeolites, through a synergetic effect between metallic and acid sites to increase the selectivity to cyclohexane [14–18]. Fluorinated beta BF was combined with a Ni/ordered mesoporous carbon to study the effect of their Brønsted acidity on the selectivity to cyclohexane (Figure 11).

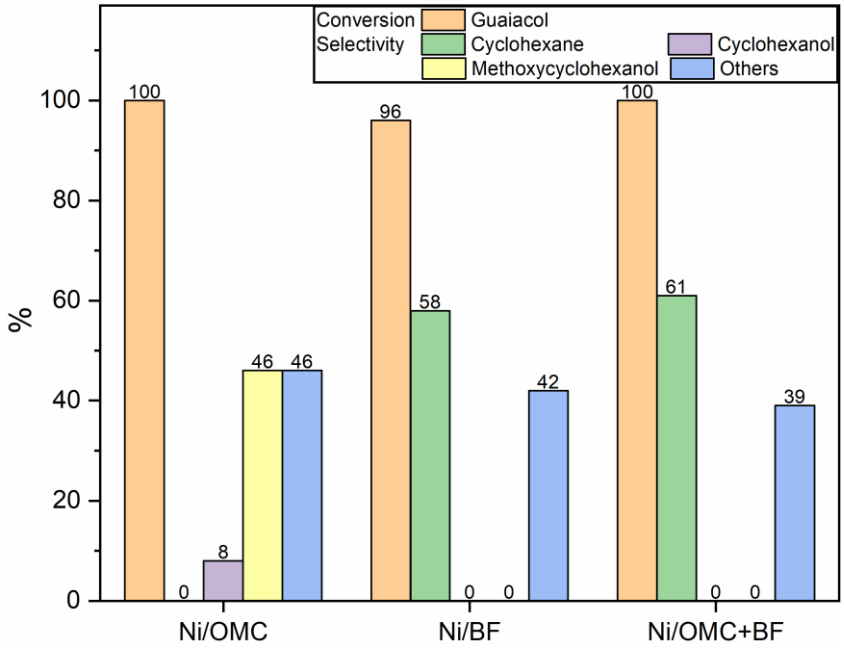

Figure 11. Catalytic activity of the Ni/OMC catalysts combined with BF. Reaction conditions: 200 mg of guaiacol; 100 mg of catalyst, for mixtures: 100 mg of Ni/OMC + 100 mg BF; H_2, 15 bar reaction time, 1 h; reaction temperature, 180 °C; solvent, dodecane.

The combination of Ni/OMC with BF led to high selectivity to cyclohexane (61%) for a total conversion compared with the Ni/OMC catalyst in which cyclohexane was not formed. Therefore, these fluorinated materials can contribute with their Brønsted acid sites as catalytic supports or as additional Brønsted acid material to the hydrodeoxygenation of guaiacol at mild conditions.

3. Materials and Methods

3.1. Materials

Na-ZSM-5 zeolite (Si/Al = 20) was purchased from EKA chemicals (Marietta, GA, USA) and NH_4-Beta zeolite (Si/Al = 12.5) from Zeoliyst international (Conshohocken, PA, USA). Ammonium fluoride (NH_4F, 95%) was purchased from Panreac Quimica SA (Barcelona, Spain); nickel(II) nitrate hexahydrate ($Ni(NO_3)_2{\cdot}6H_2O$, 98%) was purchased from Scharlau; cyclohexylamine (98%) was purchased from Aldrich (St. Louis, MO, USA); Guaiacol 98% and n-Hexadecane (99%) were purchased from Alfa Aesar Chemicals (Haverhill, MA, USA); n-dodecane (99%) was purchased from Thermo Fisher Scientific (Waltham, MA, USA). All chemicals were used as received without further purification.

3.2. Preparation of the Fluorinated Zeolites

Table 2 shows the conditions used for the fluorination of the zeolites: 1 g of commercial Na-ZSM-5 zeolite (Z) or NH_4-Beta zeolite (B) was treated with 3.5 mL of 0.05, 0.1, and 0.2 M NH_4F solution under stirring at room temperature for 42 h, following the methodology reported elsewhere [19], adapted from the methodology proposed by Borade et al. [29], obtaining samples ZF0.05, ZF, ZF0.2, BF0.05, BF, and BF0.2. In order to decrease the fluorination time, two more fluorinated samples were prepared by treating 1 g of zeolite Na-ZSM-5 with 3.5 mL of the 0.1 M NH_4F solution at 40 °C for 4 h by conventional

refluxing (ZFR) or by microwave refluxing (ZFMwR). The microwave equipment used was a Milestone FlexiWAVE laboratory apparatus working at a frequency of 2.45 GHz and equipped with a controller temperature (ATC-400). The irradiation microwave was programmed to work at a maximum of 200 W. Finally, H-Beta zeolite (HB), previously prepared by cation exchange of Na-Beta with NH_4NO_3 1 M at 100 °C for 1 h and calcined at 540 °C for 5 h, was treated with 3.5 mL of the 0.1 M NH_4F solution at room temperature for 42 h (HBF).

Table 2. Fluorination conditions of the zeolites.

Samples	[NH_4F] (M)	Treatment Temperature (°C)	Treatment Time (h)	Heating
ZF	0.1	RT	42	--
ZF0.2	0.2	RT	42	--
ZF0.05	0.05	RT	42	--
ZFR	0.1	40	4	Conventional refluxing
ZFMwR	0.1	40	4	Microwave refluxing
BF	0.1	RT	42	--
BF0.2	0.2	RT	42	--
BF0.05	0.05	RT	42	--
HBF[a]	0.1	RT	42	--

RT: Room temperature. [a] Fluorination from HB.

After fluorination, all the samples were washed with deionized water, dried in an oven at 80 °C, and pulverized using a mortar. They were then calcined under conditions of 450 °C for 8 h with a heating rate of 20 °C/min.

3.3. Preparation of the Catalysts

Fluorinated zeolites were used as supports of Ni catalysts. Thus, the supports were impregnated with an ethanolic solution containing the appropriate amounts of $Ni(NO_3)_2 \cdot 6H_2O$ to obtain 28 wt% of Ni in the final catalysts. Then, the solvent was rotary evaporated. The resulting solid was dried at 80 °C overnight, calcined in air at 450 °C for 5 h, and finally reduced under H_2 at 400 °C for 4 h (28Ni/support). Two more catalysts were prepared with ZF as a support with 10 and 20 Ni wt%, following the same methodology (10Ni/ZF adn 20Ni/ZF). The Ni/OMC catalyst was prepared as reported elsewhere [18].

3.4. Characterization Techniques

XRD (X-ray diffraction) patterns were obtained on a Siemens D5000 diffractometer (Aubrey, TX, USA) working in the Bragg–Brentano parafocusing geometry with a vertical θ–θ goniometer. This equipment is formed by a copper X-ray tube, which operating at 40 kV and 30 mA, generates the Cu Kα radiation applied to the samples, a curved graphite diffracted-beam mono chromator with diffracted-beam Soller slits, a 0.06° receiving slit, and a scintillation counter detector. Powdered samples were placed on a Si(510) sample holder. XRD patterns were collected between 2θ diffraction angles from 5 to 80°, using an angular step of 0.05° at 3 s per step with sample rotation. Crystalline phases were identified with the reference JCPDS files 65-2865-Nickel, syn-Ni; 047-1049-Bunsenite, syn-NiO; 57-0337-Beta zeolite; and 48-0074-ZSM-5 zeolite.

Elemental analyses of the samples were carried out on a Philips PW-2400 sequential XRF analyzer (Malvern, UK) using Philips Super Q v.5 software. Measures were performed in triplicate.

Langmuir surface areas were calculated from the nitrogen adsorption-desorption isotherms obtained at −196 °C using 3FLEX MICROMERITICS equipment (Norcross, GA, USA), considering the value of the cross-section of the nitrogen molecule of 0.164 nm^2. Before measurements, samples were degassed at 300 °C.

Fourier transform infrared (FTIR) spectroscopy spectra were taken on a Jasco FT/IR-6700 spectrometer (Barcelona, Spain) with a diamond crystal in the attenuated total re-

flectance mode (ATR). The frequency range used was 4000–400 cm^{-1} with a resolution of 4 cm^{-1}. Likewise, 32 scans were run and averaged to obtain a good signal-to-noise ratio.

Scanning electron microscopy (SEM) was applied to examine the morphology and particle sizes of the fluorinated samples using a JEOL JSM6400 microscope (Peabody, MA, USA), operating at accelerating voltage of 20 kV, work distance of 10.3 mm, and magnifications of 500–4000x. This equipment also has an EDX spectroscopy detector, which was used for mapping the elements present in the fluorinated samples.

^{1}H MAS-NMR (magic angle spinning nuclear magnetic resonance) spectra of fluorianted samples were recorded at room temperature using an AVANCEIII HD 600 (Bruker AXS, Rheinstetten, Germany) spectrometer with a 2.5 mm triple resonance DVT probe at a spinning rate of 25 kHz, with a 14.1 T for the magnetic field strength, corresponding to a ^{1}H resonance frequency of 600.09 MHz. The ^{1}H analysis was conducted using the One Pulse technique. The ^{1}H chemical shifts were referenced to adamantane. Spectra were recorded with a pulse width of 2.1 μs, a pulse power of 65.5 W, a delay time of 3 s, and by summing up 64 scans.

The acid content of commercial and fluorinated zeolites was quantified using the well-established procedure of thermal desorption of cyclohexylamine [36,37]. First, cyclohexylamine was added to the samples at room temperature and kept overnight under stirring. Then, the samples were dried in an oven at 80 °C for 2 h [19,34,35]. Cyclohexylamine desorption curves were obtained using Mettler Toledo TGA 2 equipment (Columbus, AL, USA), heating from 50 °C to 700 °C at a heating rate of 10 °C/min under nitrogen flow (25 mL/min). The weight loss attributed to the desorption of the cyclohexyalmine from acid sites was used to quantify the acid content of the fluorinated samples in mmol of cyclohexylamine per gram of sample [19,36,37].

3.5. Catalytic Activity Tests

The hydrodeoxygenation of guaiacol was carried out in a stainless-steel stirred autoclave (150 mL) at 180 °C and 15 bar of H_2 pressure for 1 h. Stirring was set at 700 rpm to avoid external diffusion limitations. The reactor was loaded with 200 mg of guaiacol, 40 mL of n-dodecane, and 100 mg of catalyst. In one experiment, a 100 mg of sample BF was combined by physical mixing with 100 mg of Ni/OMC.

The reaction products were identified and quantified by gas chromatography using a Shimadzu GC-2010 instrument (Tokyo, Japan) equipped with a TRB-PETROL column (100 m × 0.25 mm × 0.50 μm) and a FID detector. Hexadecane was used as the internal standard. Calibration lines were obtained from commercial products.

Author Contributions: Conceptualization, Y.C. and J.G.-R.; methodology, G.Q.-A. and A.C.R.; validation, Y.C. and J.G.-R.; investigation, G.Q.-A. and A.C.R.; resources, Y.C.; writing—original draft preparation, J.F., J.G.-R. and Y.C.; writing—review and editing, J.F., J.G.-R. and Y.C.; supervision, J.G.-R. and Y.C.; funding acquisition, Y.C. All authors have read and agreed to the published version of the manuscript.

Funding: This work was supported by the project PID2019-110735RB-C22 funded by MICIU/AEI/10.13039/501100011033. A. Rueda thanks to Generalitat de Catalunya for the FI_B 00128 grant.

Data Availability Statement: The original contributions presented in the study are included in the article; further inquiries can be directed to the corresponding author/s.

Conflicts of Interest: The authors declare no conflicts of interest. The funders had no role in the design of the study; in the collection, analyses, or interpretation of data; in the writing of the manuscript; or in the decision to publish the results.

References

1. Sheldon, R.A. Green and Sustainable Manufacture of Chemicals from Biomass: State of the Art. *Green Chem.* **2014**, *16*, 950–963. [CrossRef]
2. Broglia, F.; Rimoldi, L.; Meroni, D.; De Vecchi, S.; Morbidelli, M.; Ardizzone, S. Guaiacol Hydrodeoxygenation as a Model for Lignin Upgrading. Role of the Support Surface Features on Ni-based Alumina-silica Catalysts. *Fuel* **2019**, *243*, 501–508. [CrossRef]

3. Panwar, N.L.; Kaushik, S.C.; Kothari, S. Role of Renewable Energy Sources in Environmental Protection: A review. *Renew. Sustain. Energy Rev.* **2011**, *15*, 1513–1524. [CrossRef]
4. Park, J.; Riaz, A.; Insyani, R.; Kim, J. Understanding the Relationship Between the Structure and Depolymerization Behavior of Lignin. *Fuel* **2018**, *217*, 202–210. [CrossRef]
5. Saidi, M.; Samimi, F.; Karimipourfard, D.; Nimmanwudipong, T.; Gates, B.C.; Rahimpour, M.R. Upgrading of Lignin-derived Bio-oils by Catalytic Hydrodeoxygenation. *Energy. Environ. Sci.* **2014**, *7*, 103–129. [CrossRef]
6. Bykova, M.; Ermakov, D.; Kaichev, V.; Bulavchenko, O.; Saraev, A.; Lebedev, M. Ni-based Sol–gel Catalysts as Promising Systems for Crude Bio-oil Upgrading: Guaiacol Hydrodeoxygenation Study. *Appl. Catal. B Environ.* **2012**, *113*, 296–307. [CrossRef]
7. Huber, G.; Iborra, S.; Corma, A. Synthesis of Transportation Fuels from Biomass: Chemistry, Catalysts, and Engineering. *Chem. Rev.* **2006**, *106*, 4044–4098. [CrossRef]
8. Furimsky, E. Catalytic Hydrodeoxygenation. *Appl. Catal. A Gen.* **2000**, *199*, 147–190. [CrossRef]
9. Yan, P.; Meng-Jung, M.; Kennedy, E.; Adesina, A.; Zhao, G.; Setiawan, A.; Stockenhuber, M. The Role of Acid and Metal Sites in Hydrodeoxygenation of Guaiacol Over Ni/Beta Catalysts. *Catal. Sci. Technol.* **2020**, *10*, 810–825. [CrossRef]
10. Hellinger, M.; Carvalho, H.; Baier, S.; Wang, D.; Kleist, W.; Grunwaldt, J.D. Catalytic Hydrodeoxygenation of Guaiacol Over Platinum Supported on Metal Oxides and Zeolites. *Appl. Catal. A Gen.* **2015**, *490*, 181–192. [CrossRef]
11. Wang, Y.; Huang, H.; Baxter, N.; Liao, Y.; Zhao, Y.; Wang, S. Guaiacol Hydrodeoxygenation Over Pd Catalyst with Mesoporous ZSM-5 Support Synthesized by Solid-state Crystallization. *Catalysis. Today* **2020**, *358*, 60–67. [CrossRef]
12. Gutierrez, S.; Berenguer, A.; Prech, J.; Opanasenko, M.; Ochoa, C.; Pizarro, P.; Cejka, J.; Serrano, D.; Coronado, J.; Moreno, I. Guaiacol Hydrodeoxygenation Over Ni_2P Supported on 2D-Zeolites. *Catalysis. Today* **2020**, *345*, 48–58. [CrossRef]
13. Li, W.; Wang, H.; Wu, X.; Betancourt, L.; Tu, C.; Liao, M.; Cui, X.; Li, F.; Zheng, J.; Li, R. Ni/hierarchical ZSM-5 Zeolites as Promising Systems for Phenolic Bio-oil Upgrading: Guaiacol Hydrodeoxygenation. *J. Mater. Sci.* **2020**, *274*, 117859. [CrossRef]
14. Wang, X.; Zhu, X.; Wang, S.; He, Y.; Liu, Y.; Wang, J.; Fan, W.; Lv, Y. Low temperature hydrodeoxygenation of guaiacol into cyclohexane over Ni/SiO_2 catalyst combined with Hβ zeolite. *RSC Adv.* **2019**, *9*, 3868–3876. [CrossRef] [PubMed]
15. Qiu, S.; Xu, Y.; Weng, Y.; Ma, L.; Wang, T. Efficient Hydrogenolysis of Guaiacol over Highly Dispersed Ni/MCM-41 Catalyst Combined with HZSM-5. *Catalysts* **2016**, *6*, 134. [CrossRef]
16. Roldugina, E.A.; Naranov, E.R.; Maximov, A.L.; Karakhanov, E.A. Hydrodeoxygenation of guaiacol as a model compound of bio-oil in methanol over mesoporous noble metal catalysts. *Appl. Catal. A Gen.* **2018**, *553*, 24–35. [CrossRef]
17. Song, W.J.; Liu, Y.S.; Barath, E.; Zhao, C.; Lercher, J.A. Synergistic effects of Ni and acid sites for hydrogenation and C–O bond cleavage of substituted phenols. *Green Chem.* **2015**, *17*, 1204–1218. [CrossRef]
18. Casadó, A.; Rösch, A.; Rueda, A.C.; Uribe, A.; González, M.D.; Romero, A.J.; Carvajal, J.J.; Cesteros, Y. Catalytic potential of green ordered mesoporous carbons, obtained from biomass-derived xylose, glucose, and lignin. *Microporous Mesoporous Mater.* **2024**, *372*, 113097. [CrossRef]
19. González, M.D.; Cesteros, Y.; Salagre, P. Establishing the role of Bronsted acidity and porosity for the catalytic etherification of glycerol with tert-butanol by modifying zeolites. *Appl. Catal. A. Gen.* **2013**, *450*, 178–188. [CrossRef]
20. Imelik, B.; Vedrine, J.C. *Catalyst Characterization: Physical Techniques for Solid Materials*; Plenum Press: New York, NY, USA, 1994.
21. González, M.D.; Cesteros, Y.; Salagre, P. Comparison of Dealumination of Zeolites Beta, Mordenite and ZSM-5 by Treatment with Acid Under Microwave Irradiation. *Microporous Mesoporous Mater.* **2011**, *144*, 162–170. [CrossRef]
22. Zeng, X.; Hu, X.; Song, H.; Xia, G.; Shen, Z.; Yu, R.; Moskovits, M. Microwave Synthesis of Zeolites and Their Related Applications. *Microporous Mesoporous Mater.* **2021**, *323*, 111262. [CrossRef]
23. De Boer, J.H. *The Structure and Properties of Porous Materials*; Everett, D.H., Stone, F.S., Eds.; Butterworth: London, UK, 1958; p. 68.
24. Kral, H.; Rouquerol, J.; Sing, K.; Unger, K.K. *Characterization of Porous Solids, Studies in Surface Science and Catalysis*, 1st ed.; Elsevier: Amsterdam, The Netherlands, 1988; Volume 39, p. 101.
25. Voogd, P.; Scholten, J.J.F.; van Bekkum, H. Use of the t-plot—De Boer method in Pore Volume Determinations of ZSM-5 Type Zeolites. *Colloids Surf.* **1991**, *55*, 163–171. [CrossRef]
26. Jacobs, P.A.; Beyer, H.K.; Valyon, J. Properties of the End Members in the Pentasil-family of Zeolites: Characterization as Adsorbents. *Zeolites* **1981**, *1*, 161–168. [CrossRef]
27. Jentys, A.; Lercher, J.A. Chapter 8 Techniques of zeolite characterization. *Stud. Surf. Sci. Catal.* **2001**, *137*, 345–386. [CrossRef]
28. Jacobs, P.A.; Flanigen, E.M.; Jansen, J.C.; van Bekkum, E. *Introduction to Zeolite Science and Practice*, 2nd ed.; Elsevier: Amsterdam, The Netherlands, 2001; Volume 137, pp. 345–386.
29. Borade, R.; Clearfield, A. Effect of fluoride ions on the acidic and catalytic properties of beta zeolite. *J. Chem. Soc. Faraday Trans.* **1995**, *91*, 539–547. [CrossRef]
30. Wang, W.; Xu, J.; Deng, F. Recent advances in solid-state NMR of zeolite catalysts. *Natl. Sci. Rev.* **2022**, *9*, 155. [CrossRef]
31. Gabrienko, A.; Danilova, I.G.; Arzumanov, S.S.; Toktarev, A.V.; Freude, D.; Stepanov, A.G. Strong Acidity of Silanol Groups of Zeolite Beta: Evidence from the Studies by IR Spectroscopy of Adsorbed CO and ^{1}H MAS NMR. *Microporous Mesoporous Mater.* **2010**, *131*, 210. [CrossRef]
32. Müller, M.; Harvey, G.; Prins, R. Comparison of the dealumination of zeolites beta, mordenite, ZSM-5 and ferrierite by thermal treatment, leaching with oxalic acid and treatment with $SiCl_4$ by ^{1}H, ^{29}Si and ^{27}Al MAS NMR. *Microporous Mesoporous Mater.* **2000**, *34*, 135. [CrossRef]

33. Dongil, A.B.; Pastor-Pérez, L.; Sepúlveda-Escribano, A.; García, R.; Escalona, N. Hydrodeoxygenation of Guaiacol: Tuning the Selectivity to Cyclohexene by Introducing Ni Nanoparticles Inside Carbon Nanotubes. *Fuel* **2016**, *172*, 65–69. [CrossRef]
34. Dongil, A.B.; Ghampson, I.T.; García, R.; Fierro, J.L.G.; Escalona, N. Hydrodeoxygenation of Guaiacol Over Ni/carbon Catalysts: Effect of the Support and Ni Loading. *RSC Adv.* **2016**, *6*, 2611–2623. [CrossRef]
35. López, M.; Palacio, R.; Royer, S.; Mamede, A.S.; Fernández, J.J. Mesostructured CMK-3 Carbon Supported Ni–ZrO_2 as Catalysts for the Hydrodeoxygenation of Guaiacol. *Microporous Mesoporous Mater.* **2020**, *292*, 109694. [CrossRef]
36. Breen, C. Thermogravimetric and Infrared Study of the Desorption of Butylamine, Cyclohexylamine and Pyridine from Ni- and Co-exchanged Montmorillonite. *Clay Miner.* **1991**, *26*, 487–496. [CrossRef]
37. Mokaya, R.; Jones, W.; Moreno, S.; Poncelet, G. n-heptane Hydroconversion Over Aluminosilicate Mesoporous Molecular Sieves. *Catal. Lett.* **1997**, *49*, 87–94. [CrossRef]